REGULAR ARTICLE

blood advances

Multiomics analysis of red blood cells reveals thalassemia severity beyond globin gene mutations

Nibedita Mitra,[1,2] Upasana Bhattacharyya,[1] Prosanto Chowdhury,[1,3] Arijit Pal,[2] Arvind M. Korwar,[2] Samsidhhi Bhattacharjee,[2] and Anupam Basu[1,2,4]

[1]Department of Zoology, The University of Burdwan, Bardhaman, India; [2]BRIC-National Institute of Biomedical Genomics, Kalyani, India; [3]Peerless Hospital and B.K. Roy Research Centre, Kolkata, India; and [4]Department of Molecular Biology and Human Genetics, The University of Burdwan, Burdwan, Purbo Bardhaman, West Bengal, India

Key Points

- Interrogation of patients with the same HBB genotype reveals severity driven by dysregulated autophagy, chaperones, and ferroptosis pathways.
- Splicing dysfunction, posttranscriptional deregulation may contribute to increased disease severity in patients with TDT.

Hemoglobinopathies are the most common monogenic genetic disorders, primarily managed through blood transfusions or bone marrow transplantation. Clinical severity other than mutational effect is not well investigated and still unknown. This study aimed to identify dysregulated molecular pathways in red blood cells (RBCs) contributing to thalassemia severity. From a cohort of 285 patients with hemoglobinopathy, 10 age-matched individuals with identical compound heterozygous mutations (IVS 1-5 G>C and CD 26 G>A) were screened. Five had severe thalassemia requiring regular transfusions, whereas 5 had a nonsevere form requiring fewer transfusions. RNA sequencing and proteome analysis were conducted on isolated RBCs using NovaSeq and Orbitrap mass spectrometry platforms, respectively. Bioconductor R and different bioinformatics tools were used subsequently. Integrated transcriptome-proteome analysis revealed a global loss of messenger RNA–protein concordance. CDK11A and MCTS1 lost positive correlation, whereas RLP38 and H3C1 showed compensatory overtranslation, linked to transcription factors regulating erythropoiesis. In transfusion-dependent thalassemia (TDT), WNK3, HNRNPUL1, COPS7A, and HTATSF1 displayed discordant expression, indicating posttranscriptional aberrations. Protein-to-transcript ratio analysis showed reduced cytoskeletal (ankyrin, spectrin) expression, elevated chaperone activity, elevated ferroptosis markers (ferritin heavy chain 1, ferritin light chain, heme oxygenase-1), and suppressed autophagy. Collectively, these multilayered alterations, including splicing dysfunction, posttranscriptional deregulation, ferroptosis, autophagy suppression, oxidative stress, and cytoskeletal fragility, underlie the greater disease severity observed in TDT than non–transfusion-dependent thalassemia.

Introduction

Hemoglobinopathies are among the most common genetic disorders worldwide, carried by an estimated 300 million people, with β-thalassemia representing a substantial portion and resulting from mutations in the HBB gene that disrupt globin chain synthesis.[1] Thalassemia is classified as

Submitted 18 April 2025; accepted 13 January 2026; prepublished online on *Blood Advances* First Edition 30 January 2026. https://doi.org/10.1182/bloodadvances.2025016677.

All transcriptome data have been deposited in the National Center for Biotechnology Information Sequence Read Archive database (BioProject accession number PRJNA1074078). Proteome data been deposited in the Proteomics Identifications database (accession number PXD054385). All these data will be publicly available as per procedure.

The full-text version of this article contains a data supplement.

transfusion-dependent thalassemia (TDT), requiring regular transfusions, and non–transfusion-dependent thalassemia (NTDT), which follows a milder clinical course.

Traditionally, disease severity has been attributed to the type of β- or α-globin mutations. However, clinical variability exists even among patients with identical HBB mutations. Symptoms such as bone marrow expansion, extramedullary hematopoiesis, and hepatosplenomegaly further exacerbate disease burden.[2-5] Although blood transfusions remain the primary treatment, they are associated with iron overload, cardiotoxicity, and increased infection risk. Hydroxyurea, used to induce fetal hemoglobin, has shown limited efficacy influenced by genetic polymorphisms like Xmn1.[6]

Interestingly, patients with the same HBB genotype often present with distinct phenotypes: some require frequent transfusions (TDT), whereas others remain transfusion-independent (NTDT). This suggests that molecular factors beyond HBB mutations influence disease severity. However, the underlying mechanisms remain poorly understood, limiting therapeutic advancements.[7,8]

Given that red blood cells (RBCs) are the principal cellular targets in thalassemia, elucidating their molecular alterations is essential for understanding disease pathology; nevertheless, the transcriptional and proteomic landscapes of thalassemic RBCs have remained largely uncharacterized.[9-15] To address this gap, we used an integrated transcriptomic and proteomic (multiomics) approach using patient-derived RBCs to delineate the molecular pathways that differentiate TDT from NTDT, thereby uncovering mechanisms underlying phenotypic severity beyond the primary HBB mutations

Materials and methods

Cohort design and sample collection

A cohort of 285 patients with thalassemia (aged 8-20 years) with the β^0/β^+ genotype was screened using stringent inclusion criteria.

Unlike other genotypes, such as β^0/β^0 or β^+/β^+, the β^+/β^0 genotype exhibits a phenotypic dichotomy, presenting both severe and nonsevere clinical manifestations. Thus, this genotype serves as an ideal experimental model for investigating the causes of disease severity beyond the pathogenic effects of mutations.

To ensure a homogeneous genotype among patients, we excluded other known genetic variants that influence thalassemia severity, such as mutations in the α-globin gene or the fetal hemoglobin–inducing Xmn1/γ^G-globin 185 C>T polymorphism. From this group, patients with identical HBB genotypes (IVS 1-5 G>C and CD 26 G>A), matched for age and sex, were selected for multiomics investigation (Table 1). From this cohort, 10 patients were selected for transcriptomic and proteomic analysis. Following the Thalassaemia International Federation guidelines,[16] 5 patients were classified as TDT, requiring transfusions every 2 to 3 months, whereas 5 were categorized as NTDT, not requiring frequent transfusions. Clinical details are presented in supplemental Table 1. In addition, 5 age-matched healthy donors served as controls.

In the severe group, patients exhibited symptoms early in life (<12 months) with low hemoglobin levels (6-7.5 g/dL) and required regular blood transfusions approximately every 2 months.

Table 1. Study cohort information

	Total β^+/β^0 subset (N = 285)	Omics subset with β^+/β^0 genotype	
		Severe patients (n = 5)	Nonsevere patients (n = 5)
Ethnicity	Bengali, Indian	Bengali, Indian	Bengali, Indian
Average age, y	7	12	13.8
Gender, M/F, %	40/60	40/60	20/80
Mean Hb, g/dL	6.7	6.4	7.6
HbF, %	31.1	37.6	38.3
MCV, fL	68.03	60.64	71.2
MCH (pg/cell)	19.8	18.88	22.3
β genotype (β^0/β^+)	All	All	All
Secondary modifier (α genotype), %	12	NIL	NIL
Xmn1/γ^G-globin 185 C>T, %	30	NIL	NIL
Average transfusion interval, mo	3.6	2.0	12 or no transfusion
Splenectomy, %	13	NIL	NIL
Median serum ferritin, ng/mL	555	1061	330

F, female; Hb, hemoglobin; HbF, fetal hemoglobin; M, male; MCH, mean corpuscular hemoglobin; MCV, mean corpuscular volume.

These patients underwent biochemical screening for iron overload (serum ferritin) and received regular iron chelation therapy.

The nonsevere group comprised 5 patients who developed anemia at a later age and required fewer transfusions, with an average hemoglobin level of 7 to 8 g/dL. Given that their serum ferritin levels indicated that iron overload remained within tolerable limits, they were not placed on regular iron chelation therapy (supplemental Table 1).

Peripheral blood (4.5-5 mL) was collected in EDTA vials.

Sex as a biological variable

The study included both male and female participants to minimize sex-related bias. Among the severe (TDT) group, there were 2 males and 3 females, whereas the nonsevere (NTDT) group included 1 male and 4 females. The control group comprised 2 males and 3 females.

RBC isolation and RNA extraction

RBCs were isolated using density gradient centrifugation. RNA was extracted using the TRIzol Plus RNA Purification Kit (Invitrogen, catalog no. 12183555) and assessed for quality and quantity via spectrophotometry and electrophoresis.

RNA-seq and data analysis

RNA sequencing (RNA-seq) libraries were prepared using the KAPA RNA HyperPrep Kit (Kapa Biosystems, catalog no. KK8561) and sequenced on the NovaSeq 6000 Illumina platform (2 × 100 base pair read length, targeting 75 million reads per sample) at the National Institute of Biomedical Genomics Facility. Quality control checks, adapter trimming, and read alignment to the hg38 reference genome were performed using Illumina

DRAGEN v4. Binary alignment map files were processed to generate gene expression counts, and differential gene expression (DGE) analysis was conducted using DESeq2. Significance thresholds were set at a $\log_2$ fold change ($\log_2$FC) >1 or less than −1 and an adjusted $P < .05$. Noncoding RNA transcripts were annotated using BioMart (Ensembl).

RBC proteomics sample preparation

A 75 μL RBC suspension was used for protein extraction with a radioimmunoprecipitation assay buffer (Thermo Fisher Scientific), and hemoglobin was depleted using the HemoVoid Kit (Biotech Support Group, catalog no. HVB-MS10). Protein concentration was measured using the bicinchoninic acid assay kit (Thermo Fisher Scientific). A total of 200 μg of protein was processed in ammonium bicarbonate buffer, reduced with dithiothreitol, alkylated with iodoacetamide, and digested with trypsin at 37°C for 18 hours. We performed label-free comparative quantitative proteomics using a total of 15 biological samples. These included 5 control participants, 5 patients with TDT, and 5 patients with NTDT. For each participant, RBC lysates were prepared and analyzed as independent biological replicates. Each biological replicate was further analyzed in triplicate to generate 3 technical replicates for the proteomic study.

Liquid chromatography–MS/MS analysis

The liquid chromatography–mass spectrometry (MS)/MS platform was set up as described in a previous study.[17] Liquid chromatography–MS/MS was performed using an RSLCnano system coupled to a Q Exactive Plus Orbitrap mass spectrometer. Peptide digests (750 ng) were separated on a C18 column using gradient elution. Data-dependent MS/MS acquisition was conducted in positive-ion mode. Proteomic data were processed using SEQUEST HT within Proteome Discoverer 2.4 and mapped to the UniProt human database. Given that the proteome quantification was comparative, the database search for protein identification was performed simultaneously for all 45 replicates (15 × 3) with a single analytical workflow for reliable comparison. Furthermore, to assure a higher-quality proteomic data set, the samples were acquired in 3 batches. Standard HeLa digest was acquired at the beginning and after every 15 samples. The number of proteins and the number of peptide-spectrum matches corresponding to each protein in HeLa digest were consistent across 3 batches, assuring a higher-quality data set without any batch effect. Small nuclear ribonucleoproteins (snRNPs) were manually filtered using the UniProt snRNP database. Differential protein abundance between healthy controls vs thalassemia and TDT vs NTDT groups was analyzed using DEqMS in R.

Integration of transcriptome and proteome data

To integrate transcriptomic and proteomic readouts, we computed Pearson correlation coefficients for each matched transcript-protein pair separately within the thalassemia and control groups and between the TDT and NTDT subgroups. Significant differences in these correlations between groups were assessed using the R package cocor,[18] which enables statistical comparison of independent correlation coefficients.

Subsequently, the protein-to-transcript ratio (PTR) for each matched gene-protein pair was calculated as $\log_2$(protein abundance) − $\log_2$(transcript abundance). PTR values were analyzed using the limma linear modeling workflow, in which a design matrix was constructed to encode the comparisons between thalassemia vs control and TDT vs NTDT. Differential PTR estimates ($\log_2$FC in PTR) and corresponding P values were obtained using empirical Bayes moderation as described previously.[19-21]

Statistical and bioinformatics analysis

Statistical analyses were conducted using Bioconductor R. Sample size power estimation was performed using an online RNA-seq power calculation tool. A Student t test ($P < .05$) was applied for box plot analysis of key differentially expressed proteins between TDT and NTDT groups. Gene set enrichment analysis (GSEA) was performed using the clusterProfiler 3.16 package to identify functional pathways. Additional bioinformatics analyses included Gene Ontology (GO) analysis using ShinyGO, disease ontology enrichment using Metascape 2.0[22] and EnrichR, and protein-protein interaction analysis using STRING.

Ethical approval

The study was approved by the Institutional Clinical Ethics Committee of The University of Burdwan (approval no. IEC/BU/2021/10) and conducted as per the World Medical Association Declaration of Helsinki. A written informed consent was obtained from all participants as part of a multicentric project, ensuring no interference with patient care.

Results

Transcriptome profile

DEG between patients with thalassemia and control participants. Principal component analysis (PCA) and cluster heat map analysis of the RBC transcriptome revealed distinct heterogeneity between patients and controls. We identified 2612 differentially expressed genes (DEGs) in patients with thalassemia compared with controls, based on a $\log_2$Fc >2 or less than −2 and adjusted P (false discovery rate [FDR]) < .05 (supplemental File 1; supplemental Figure 2A-C; supplemental Table 1). To explore the functional enrichment of DEGs in RBCs of patients with thalassemia, GO molecular functions and pathway enrichment analyses were conducted. GSEA demonstrated that the highest positive enrichment was observed in ATP-dependent protein-folding chaperones, with a normalized enrichment score of 3.01 (Figure 1A). The upregulated gene sets in thalassemia further showed enrichment in hemoglobin α binding, hemoglobin binding, haptoglobin binding, oxygen carrier activity, oxidoreductase activity, peroxidase activity, unfolded protein binding, and chaperone binding activity (supplemental File 1; supplemental Figure 2D). Kyoto Encyclopedia of Genes and Genomes (KEGG) pathway enrichment analysis revealed that the upregulated DEGs were associated with ferroptosis (supplemental File 1; supplemental Figure 2E). In contrast, the downregulated gene sets in RBCs from patients with thalassemia were significantly enriched in immunoglobulin G binding, interleukin-1 receptor binding, pattern recognition receptor binding, phosphotyrosine residue binding, phosphoprotein binding, actin filament binding, and actin binding (supplemental File 1; supplemental Figure 2F).

DEG between patients with TDT and NTDT. Comparative transcriptome analysis between TDT and NTDT revealed distinct

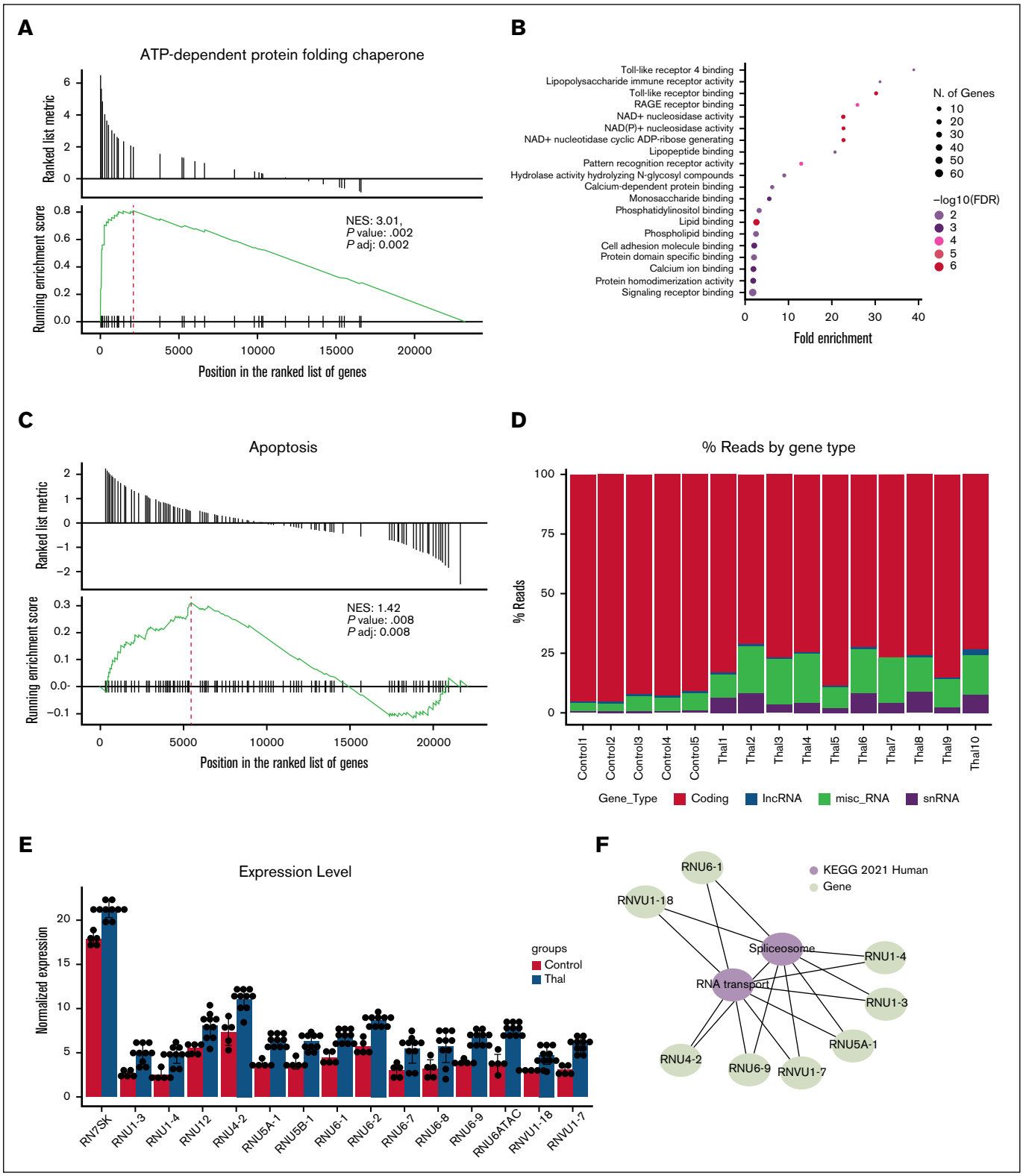

Figure 1. Findings of transcriptome. (A) GSEA of KEGG pathways revealed significant upregulation of the ATP-dependent protein-folding chaperone pathway in thalassemia (NES = 3.01; *P* adj < .002). (B) GO molecular function (GOMF) analysis showing enriched molecular functions among genes upregulated in TDT samples. (C) GSEA of KEGG pathways demonstrated dysregulation of apoptosis-related genes in TDT compared with NTDT normalized enrichment score (NES = 1.42; *P* adj < .02). (D) Relative percentage of reads of different types of RNAs found in control (n = 5) and thalassemia (n = 10): an increased proportion of snRNA reads (violet bars) in thalassemia. (E) Expression of different snRNAs in thalassemia and control samples. (F) Functional enrichment analysis of the upregulated snRNAs in thalassemia.

molecular differences. PCA and cluster heat map analysis demonstrated significant variations in the transcriptomic profiles of RBCs between these 2 groups (supplemental File 1; supplemental Figure 3A-B; supplemental Table 2).

A total of 579 DEGs were identified between patients with TDT and NTDT, as depicted in the volcano plot (supplemental File 1; supplemental Figure 3C). These genes represent key molecular players potentially contributing to the differences in disease severity and clinical manifestations between the 2 thalassemia subtypes.

To explore factors contributing to the increased severity in patients with TDT, we performed a detailed analysis of gene expression profiles. Transcriptome data revealed that upregulated genes in the TDT group were significantly enriched in molecular functions related to Toll-like receptor (TLR) and receptor for advanced glycation end products (RAGE) binding activity (Figure 1B). These findings suggest an enhanced inflammatory and immune response in TDT, which may exacerbate disease severity.

Conversely, downregulated genes in the TDT group were predominantly associated with cytoskeletal protein membrane anchor activity (supplemental File 1; supplemental Figure 3D). This downregulation may indicate compromised RBC structural integrity, potentially leading to reduced life span and increased susceptibility to hemolysis in patients with TDT.

GSEA further highlighted contrasting pathway activations between the 2 groups. In patients with TDT, genes involved in the apoptosis pathway were significantly upregulated (Figure 1C), suggesting an increased rate of programmed cell death that may accelerate RBC turnover. In contrast, genes associated with the hematopoietic cell lineage pathway were downregulated (supplemental File 1; supplemental Figure 3E), implying impaired erythropoiesis and a reduced capacity for effective RBC production in TDT.

Collectively, these findings provide insights into the molecular mechanisms underlying the greater clinical severity of TDT than NTDT. The upregulation of inflammatory and apoptotic pathways, along with the downregulation of structural and hematopoietic functions, likely contributes to the increased transfusion dependency and overall disease burden in patients with TDT.

snRNA profile

Transcriptome analysis of RBCs from both healthy individuals and patients with thalassemia revealed an intriguing trend: the thalassemia group exhibited a higher percentage of reads corresponding to small nuclear RNAs (snRNAs) than the control group (Figure 1D). Further investigation identified 15 snRNAs that were significantly upregulated in RBCs derived from patients with thalassemia (Figure 1E). However, no significant differential expression of snRNAs was observed between the 2 thalassemia subgroups.

Functional enrichment analysis of the upregulated snRNAs using KEGG pathway analysis indicated that the snRNAs RNU5A-1, RNU6-9, RNU6-1, RNVU1-7, RNVU1-18, RNU4-2, RNU1-3, and RNU1-4 were involved in the spliceosome. In addition, these snRNAs were implicated in RNA transport (Figure 1F).

Proteome profile

Differential protein abundance between patients with thalassemia and control participants. From the MS data analysis, a total of 2328 proteins were considered across all 45 replicates and subsequent normalization, of which 2211 proteins were quantified with high-confidence protein FDR and 116 with medium- and low-confidence protein FDR. In each sample, a total of 2328 proteins are quantified, which have at least 1 unique peptide being identified and a minimum positive SEQUEST HT score of 1.61.

From these 2328 proteins, 826 showed significant differences in abundance ($P < .05$; $\log_2$FC, >1 or less than −1) between patients with thalassemia and controls (supplemental Table 3). PCA and cluster heat map analysis revealed distinct clustering between the thalassemia and control groups (supplemental File 1; supplemental Figure 4A-C). The MS proteomics data have been deposited in the ProteomeXchange Consortium via the Proteomics Identifications[23] partner repository with the data set identifier PXD054385.

GO molecular function fold enrichment analysis of the proteomics data indicated that the highly abundant proteins were enriched for translation, RNA-binding, and unfolded protein-binding functions (Figure 2A). GSEA revealed that the upregulated proteins in the thalassemia group were involved in RNA degradation and mRNA surveillance pathways (Figure 2B-C). Conversely, low-abundance proteins in thalassemia were associated with haptoglobin binding, antioxidant activity, actin binding, and actin filament binding (supplemental File 1; supplemental Figure 4D).

STRING analysis showed that the highly abundant proteins were associated with chaperones and formed networks with HSPAB, HSPA1B, and DNAJB4 (supplemental File 1; supplemental Figure 4E). In contrast, low-abundance proteins were linked to cellular detoxification pathways, particularly those associated with hemolytic anemia (supplemental File 1; supplemental Figure 4F). Metascape analysis of the low-abundance proteins also indicated significant enrichment for anemia and RBC disorder–related diseases in thalassemia (supplemental File 1; supplemental Figure 4G).

Differential protein abundance between patients with TDT and NTDT. PCA revealed a 43% variance at PC1 between the TDT and NTDT groups, highlighting distinct proteomic differences (supplemental Table 4). A total of 430 differentially abundant proteins were identified between the 2 groups (supplemental File 1; supplemental Figure 5A-C).

Functional enrichment analysis revealed that proteins with higher abundance in TDT were significantly associated with TLR and RAGE binding activity (Figure 2D), suggesting a role in inflammatory signaling. In contrast, proteins with lower abundance in TDT were enriched in hemoglobin α binding, haptoglobin binding, oxygen carrier activity, protein-folding chaperone activity, and oxygen binding (supplemental File 1; supplemental Figure 5D), indicating potential impairments in RBC function and stability.

KEGG pathway analysis further demonstrated that low-abundance proteins in TDT were involved in autophagy and mitophagy

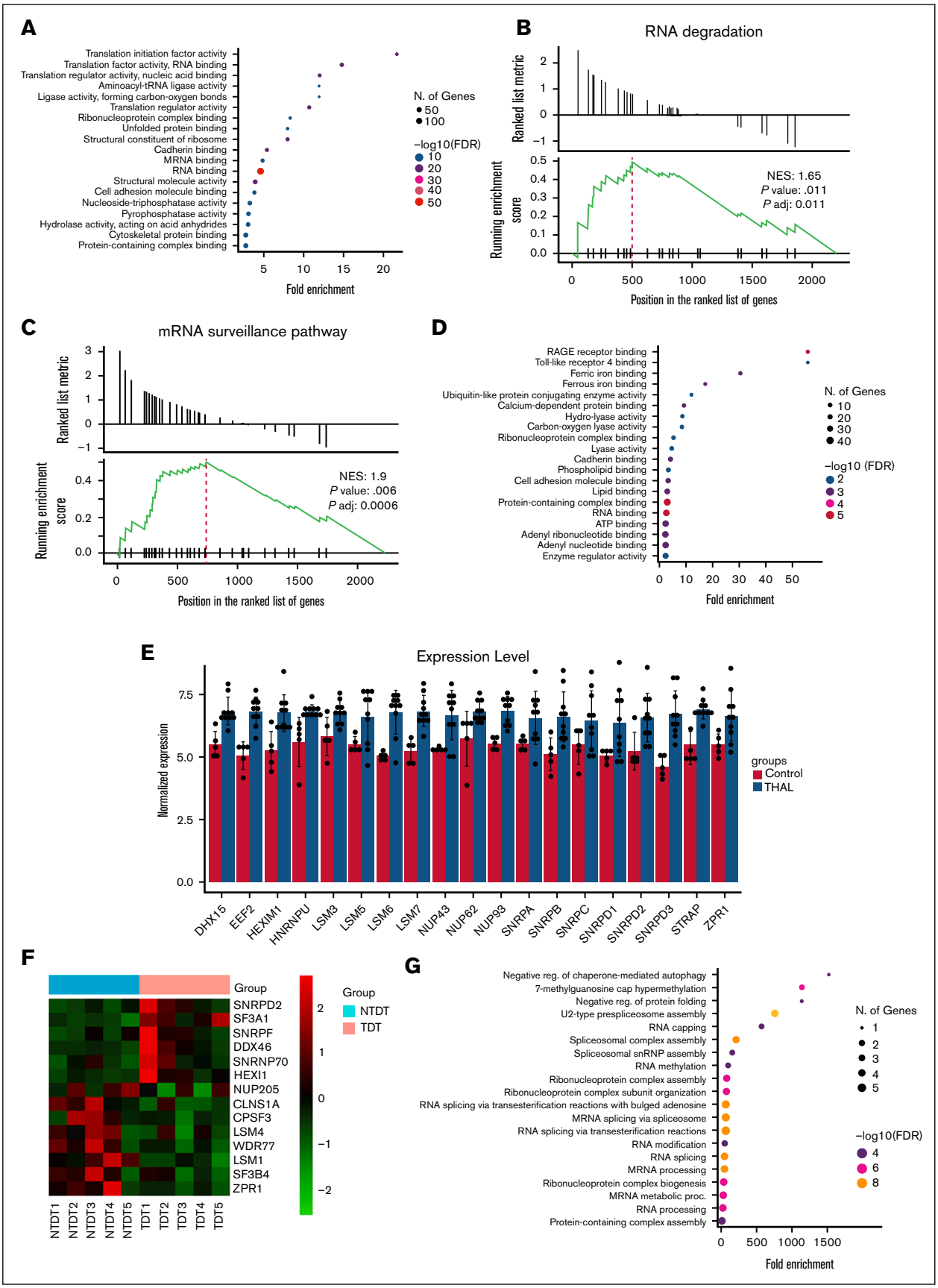
A
Translation initiation factor activity
Translation factor activity, RNA binding
Translation regulator activity, nucleic acid binding
Aminoacyl-tRNA ligase activity
Ligase activity, forming carbon-oxygen bonds
Translation regulator activity
Ribonucleoprotein complex binding
Unfolded protein binding
Structural constituent of ribosome
Cadherin binding
MRNA binding
RNA binding
Structural molecule activity
Cell adhesion molecule binding
Nucleoside-triphosphatase activity
Pyrophosphatase activity
Hydrolase activity, acting on acid anhydrides
Cytoskeletal protein binding
Protein-containing complex binding
5 10 15 20
Fold enrichment
N. of Genes
50
100
−log10(FDR)
10
20
30
40
50
B
RNA degradation
Ranked list metric
Running enrichment score
NES: 1.65
P value: .011
P adj: 0.011
0 500 1000 1500 2000
Position in the ranked list of genes
C
mRNA surveillance pathway
Ranked list metric
Running enrichment score
NES: 1.9
P value: .006
P adj: 0.0006
0 500 1000 1500 2000
Position in the ranked list of genes
D
RAGE receptor binding
Toll-like receptor 4 binding
Ferric iron binding
Ferrous iron binding
Ubiquitin-like protein conjugating enzyme activity
Calcium-dependent protein binding
Hydro-lyase activity
Carbon-oxygen lyase activity
Ribonucleoprotein complex binding
Lyase activity
Cadherin binding
Phospholipid binding
Cell adhesion molecule binding
Lipid binding
Protein-containing complex binding
RNA binding
ATP binding
Adenyl ribonucleotide binding
Adenyl nucleotide binding
Enzyme regulator activity
0 10 20 30 40 50
Fold enrichment
N. of Genes
10
20
30
40
−log10 (FDR)
2
3
4
5
E
Expression Level
Normalized expression
groups
Control
THAL
DHX15 EEF2 HEXIM1 HNRNPU LSM3 LSM5 LSM6 LSM7 NUP43 NUP62 NUP93 SNRPA SNRPB SNRPC SNRPD1 SNRPD2 SNRPD3 STRAP ZPR1
F
Group
NTDT
TDT
SNRPD2
SF3A1
SNRPF
DDX46
SNRNP70
HEXI1
NUP205
CLNS1A
CPSF3
LSM4
WDR77
LSM1
SF3B4
ZPR1
NTDT1 NTDT2 NTDT3 NTDT4 NTDT5 TDT1 TDT2 TDT3 TDT4 TDT5
G
Negative reg. of chaperone-mediated autophagy
7-methylguanosine cap hypermethylation
Negative reg. of protein folding
U2-type prespliceosome assembly
RNA capping
Spliceosomal complex assembly
Spliceosomal snRNP assembly
RNA methylation
Ribonucleoprotein complex assembly
Ribonucleoprotein complex subunit organization
RNA splicing via transesterification reactions with bulged adenosine
MRNA splicing via spliceosome
RNA splicing via transesterification reactions
RNA modification
RNA splicing
MRNA processing
Ribonucleoprotein complex biogenesis
MRNA metabolic proc.
RNA processing
Protein-containing complex assembly
0 500 1000 1500
Fold enrichment
N. of Genes
1
2
3
4
5
−log10(FDR)
4
6
8

Figure 2.

pathways (supplemental File 1; supplemental Figure 5E), suggesting disruptions in cellular homeostasis. STRING network analysis identified ferritin heavy chain 1 (FTH1) and ferritin light chain (FTL) as significantly more abundant in TDT than NTDT, linking them to the ferroptosis pathway and indicating increased iron storage in patients with TDT (supplemental File 1; supplemental Figure 5F)

Altered expression of snRNPs in RBC of thalassemia and control, as well as TDT and NTDT. Analysis of the RBC proteome identified 72 proteins classified as snRNPs based on the UniProt database. Among these, 22 snRNPs exhibited altered expression, with 19 upregulated in patients with thalassemia (Figure 2E; supplemental Table 5). These snRNPs, including snRNPs and U1-U6 snRNA-associated Sm-like proteins, were highly enriched in posttranscriptional modification regulation and snRNP binding. KEGG pathway analysis further revealed their involvement in the spliceosome and RNA degradation pathways (supplemental File 1; supplemental Figure 6A-C).

In addition, 14 proteins associated with spliceosome function and mRNA processing exhibited differential expression in patients with TDT compared with those with NTDT (Figure 2F). Among these, 6 snRNPs were upregulated in TDT, showing enrichment in pathways related to the negative regulation of autophagy, methylation processes, and protein folding. Conversely, 8 snRNPs were downregulated in TDT, implicating them in splicing regulation, splice site selection, polyadenylation, and mRNA decay (Figure 2G).

Transcriptome-proteome integrated findings

Integrated analysis of transcriptomic and proteomic data from patients with thalassemia and control participants identified 2171 proteins corresponding to RNA-seq transcripts. After removing duplicates and aligning UniProt accession numbers, 2144 matched RNA-protein pairs were retained for downstream integration (supplemental Table 6; Figure 3A).

Correlation analysis using the cocor.indep function in R revealed distinct patterns between the thalassemia and control groups. Although controls exhibited a broad distribution of positive and negative RNA-protein correlations, thalassemia samples showed a bell-shaped density centered near zero (Figure 3B), indicating a global loss of transcript-protein concordance. A total of 124 genes showed significant correlation changes (Fisher $P < .05$) (supplemental Table 6). Volcano plots highlighted genes with the largest differential correlations (Figure 3C).

Notably, CDK11A and MCTS1 displayed strong positive RNA-protein correlations ($r \approx 0.95$-0.99) in controls but lost this coherence in thalassemia, whereas RLP38 and H3C1 shifted from negative to positive correlations ($r \approx -0.95$ to 0.7). Fisher z tests confirmed the robustness of these shifts ($P < .002$), reflecting extensive posttranscriptional dysregulation.

Functionally, anticorrelated genes were enriched in proteasomal degradation, metabolism, AMP-activated protein kinase and hypoxia-inducible factor 1 signaling, and immune pathways (Figure 4A). Motif enrichment linked these discordant genes to transcription factors ER81, ERM, ELK1, E2F4, TEL1, YY1, and Sp1 (Figure 4B-C), suggesting that impaired transcription factor regulation and mRNA-protein decoupling contribute to disrupted proteostasis and disease severity in thalassemia.

Correlation analysis: TDT vs NTDT. In comparison with TDT with NTDT group, 84 genes were identified with significant correlation changes (Fisher $P < .05$). The volcano plot showed the most significantly differentially correlated genes among TDT and NTDT groups (supplemental Table 6; Figure 3H). Genes such as WNK3, HNRNPUL1, HTATSF1, UBL7, SAR1B, NUDCD1, and COPS7A showed negative Fisher z scores; their transcript-protein correlations are weaker or inverse in TDT than NTDT.

This suggests that in patients with TDT, who experience more severe ineffective erythropoiesis and oxidative stress, post-transcriptional dysregulation disrupts normal coupling between mRNA abundance and protein output.

PTR analysis. Using the limma linear model, PTRs were compared between the thalassemia and control groups. Based on cutoffs of $|\log_2 FC| > 1$ or < -1 and adjusted $P < .05$, 647 genes exhibited high PTRs and 143 genes showed low PTRs in thalassemia, reflecting altered mRNA-protein coordination (supplemental Table 7). A heat map showing the distinguishing pattern of low and high PTR RNA-protein gene signature (Figure 5A). The low PTR genes are associated with ankyrin- and spectrin-associated cytoskeleton, whereas the high PTR genes are associated with mostly RNA-binding proteins and the translational machinery (Figure 5B-C). Many of these proteins were ribosomal proteins, reflecting the occurrence of ribosomopathy in thalassemia (Figure 5D).

Similarly, PTR analysis between TDT and NTDT revealed 159 significantly altered genes ($P < .05$), with 112 showing higher and 47 showing lower PTRs in TDT. A heat map showing the top 80 genes with high and low PTRs (supplemental Table 7; Figure 6A). The low PTR genes were associated with autophagy and protein degradation pathway, whereas high PTR proteins were associated with ferroptosis, necroptosis, and others (Figure 6B-C). K-means cluster differential of these proteins was also analyzed (Figure 6D).

Discussion

The present integrative transcriptomic and proteomic analysis provides new insights into the molecular mechanisms underlying phenotypic severity in β-thalassemia, particularly between patients with TDT and NTDT sharing the same β^+/β^0 genotype. By maintaining a homogeneous genetic background and excluding known modifiers (eg, α-globin variants and Xmn1 polymorphism), this

Figure 2. Findings of proteome data. (A) GOMF analysis of highly abundant proteins in thalassemia. (B-C) GSEA revealed upregulation of RNA degradation and mRNA surveillance pathways in thalassemia compared with controls (NES = 1.65 and 1.90; P adj $< .02$). (D) GOMF analysis of highly abundant proteins in the TDT subgroup. (E) Significantly increased abundance of snRNPs in thalassemia samples. (F) Differential expression of snRNPs between TDT and NTDT groups. (G) KEGG pathway enrichment analysis of significantly altered snRNPs in TDT samples.

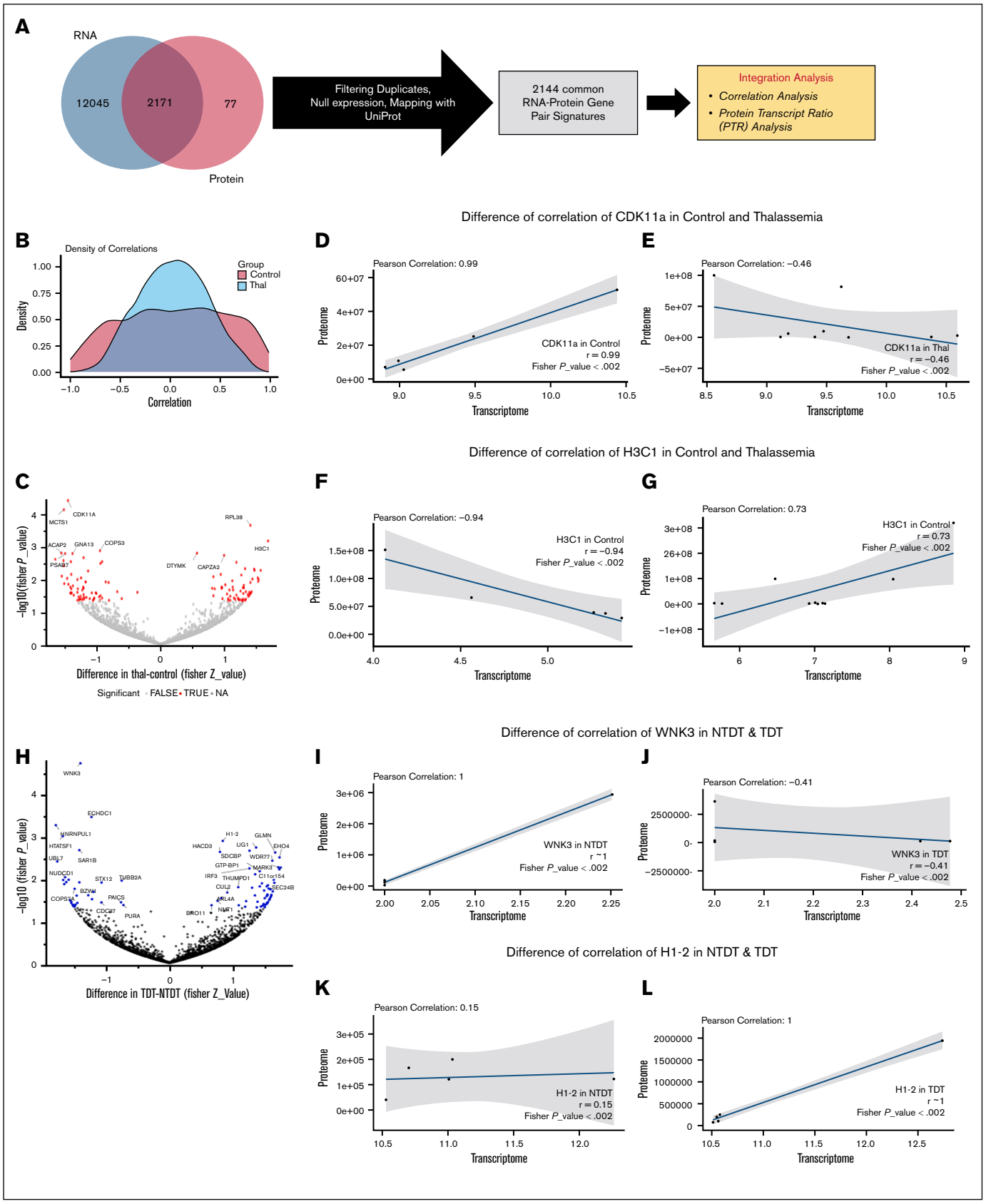
A
RNA
12045
2171
77
Protein
Filtering Duplicates, Null expression, Mapping with UniProt
2144 common RNA-Protein Gene Pair Signatures
Integration Analysis
• Correlation Analysis
• Protein Transcript Ratio (PTR) Analysis
B
Density of Correlations
Group
Control
Thal
Density
Correlation
C
−log10(fisher P_value)
Difference in thal-control (fisher Z_value)
Significant FALSE TRUE NA
Difference of correlation of CDK11a in Control and Thalassemia
D
Pearson Correlation: 0.99
CDK11a in Control
r = 0.99
Fisher P_value < .002
Proteome
Transcriptome
E
Pearson Correlation: −0.46
CDK11a in Thal
r = −0.46
Fisher P_value < .002
Proteome
Transcriptome
Difference of correlation of H3C1 in Control and Thalassemia
F
Pearson Correlation: −0.94
H3C1 in Control
r = −0.94
Fisher P_value < .002
Proteome
Transcriptome
G
Pearson Correlation: 0.73
H3C1 in Control
r = 0.73
Fisher P_value < .002
Proteome
Transcriptome
H
−log10 (fisher P_value)
Difference in TDT-NTDT (fisher Z_Value)
Difference of correlation of WNK3 in NTDT & TDT
I
Pearson Correlation: 1
WNK3 in NTDT
r ~1
Fisher P_value < .002
Proteome
Transcriptome
J
Pearson Correlation: −0.41
WNK3 in TDT
r = −0.41
Fisher P_value < .002
Proteome
Transcriptome
Difference of correlation of H1-2 in NTDT & TDT
K
Pearson Correlation: 0.15
H1-2 in NTDT
r = 0.15
Fisher P_value < .002
Proteome
Transcriptome
L
Pearson Correlation: 1
H1-2 in TDT
r ~1
Fisher P_value < .002
Proteome
Transcriptome

Figure 3.

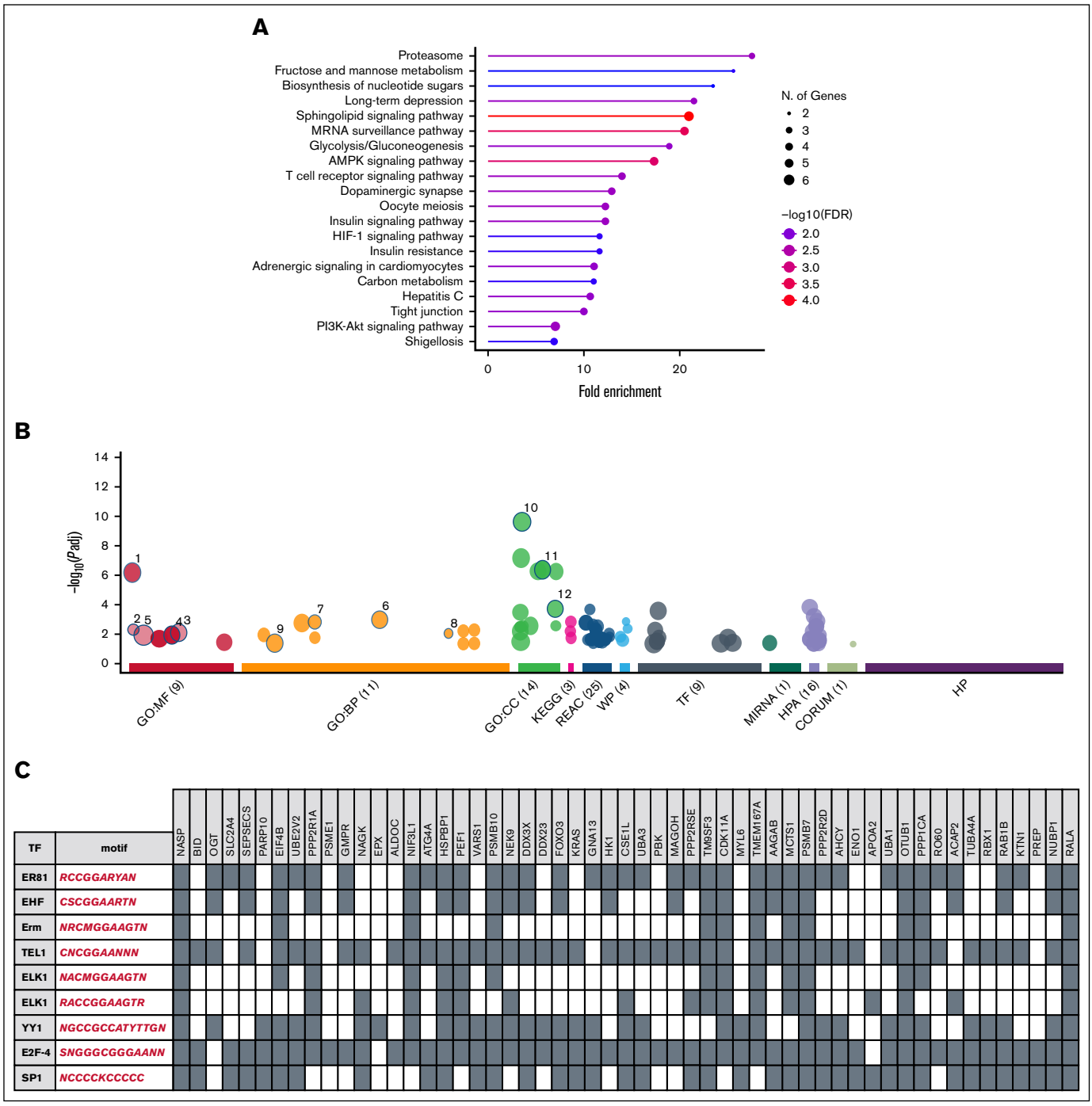

Figure 4. Enrichment analysis of anticorrelated RNA-protein gene signatures in thalassemia. (A) KEGG pathway enrichment analysis of anticorrelated RNA-protein gene signatures in thalassemia, highlighting the major pathways involved. (B) Enrichment analysis identifying 9 transcription factors associated with the anticorrelated RNA-protein gene set in thalassemia. (C) Predicted transcription factors and their target DNA-binding motifs linked to the anticorrelated gene network in thalassemia. AMPK, AMP-activated protein kinase; HIF-1, hypoxia-inducible factor 1.

Figure 3. Integration of transcriptome and proteome data. (A) Workflow showing identification of common RNA-protein gene pairs from transcriptomic and proteomic data sets for integrative analysis. (B) Density correlation plots generated using the cocor R package revealed a marked loss of transcriptome-proteome correlation in thalassemia compared with controls. (C) Volcano plot displaying differentially correlated genes between the thalassemia and control groups. (D-E) Representative example showing altered RNA-protein correlation of CDK11A, with $r \approx 1$ in controls and $r = -0.46$ in thalassemia ($P < .002$, Fisher z test). (F-G) Inverse correlation of H3C1 between control ($r = -0.94$) and thalassemia ($r = 0.73$; $P < .002$). (H) Volcano plot summarizing the top significantly altered gene correlations between TDT and NTDT samples. (I-J) Differential RNA-protein correlation of WNK3 between NTDT ($r = 1$) and TDT ($r = -0.41$; $P < .002$). (K-L) Altered correlation of H1-2 between NTDT ($r = 0.15$) and TDT ($r = 1$; $P < .002$).

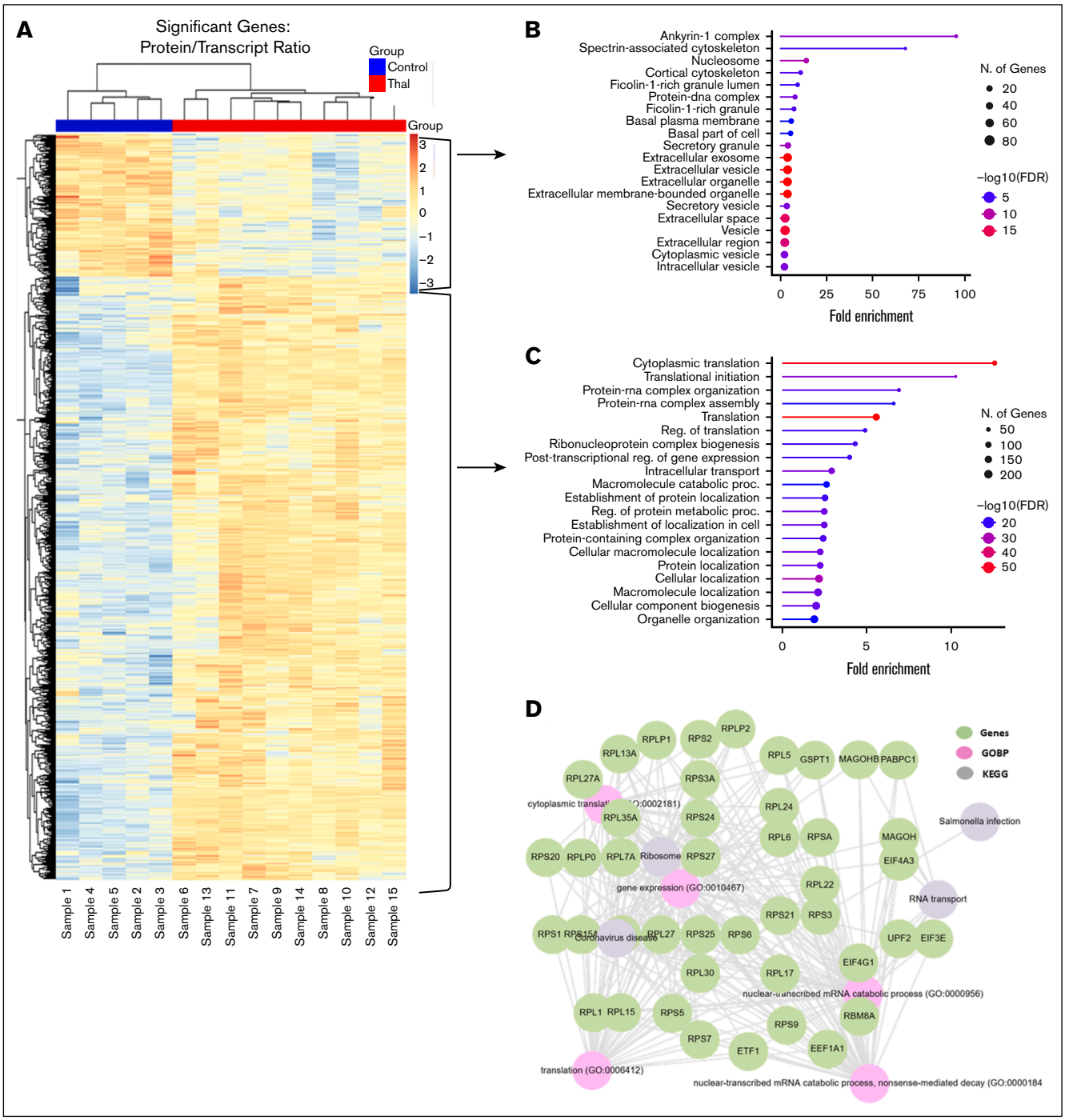

Figure 5. PTR analysis in thalassemia vs control samples. (A) Heat map showing hierarchical clustering of significant gene pairs based on low and high PTRs. (B-C) KEGG pathway enrichment analysis of genes with low and high PTRs, illustrating distinct functional pathway associations. (D) Enrichment analysis identifying ribosomal subunit proteins among high PTR gene signatures in thalassemia.

study demonstrates that disease severity in β-thalassemia primarily arises from differential molecular regulation beyond the primary HBB mutations.

At the transcriptome level, thalassemic RBCs exhibited strong upregulation of stress-related molecular chaperones (HSP90AB1, HSPH1, FKBP4), γ-globin genes (HBG1, HBG2), and ferroptosis-associated transcripts, reflecting oxidative stress, hemoglobin instability, and compensatory erythroid stress responses. These findings align with earlier reports showing increased unfolded protein load, proteostasis imbalance, and oxidative damage in β-thalassemic erythroid cells.[24-26] GO enrichment for unfolded protein binding and oxidoreductase activity further suggests activation of cytoprotective chaperone

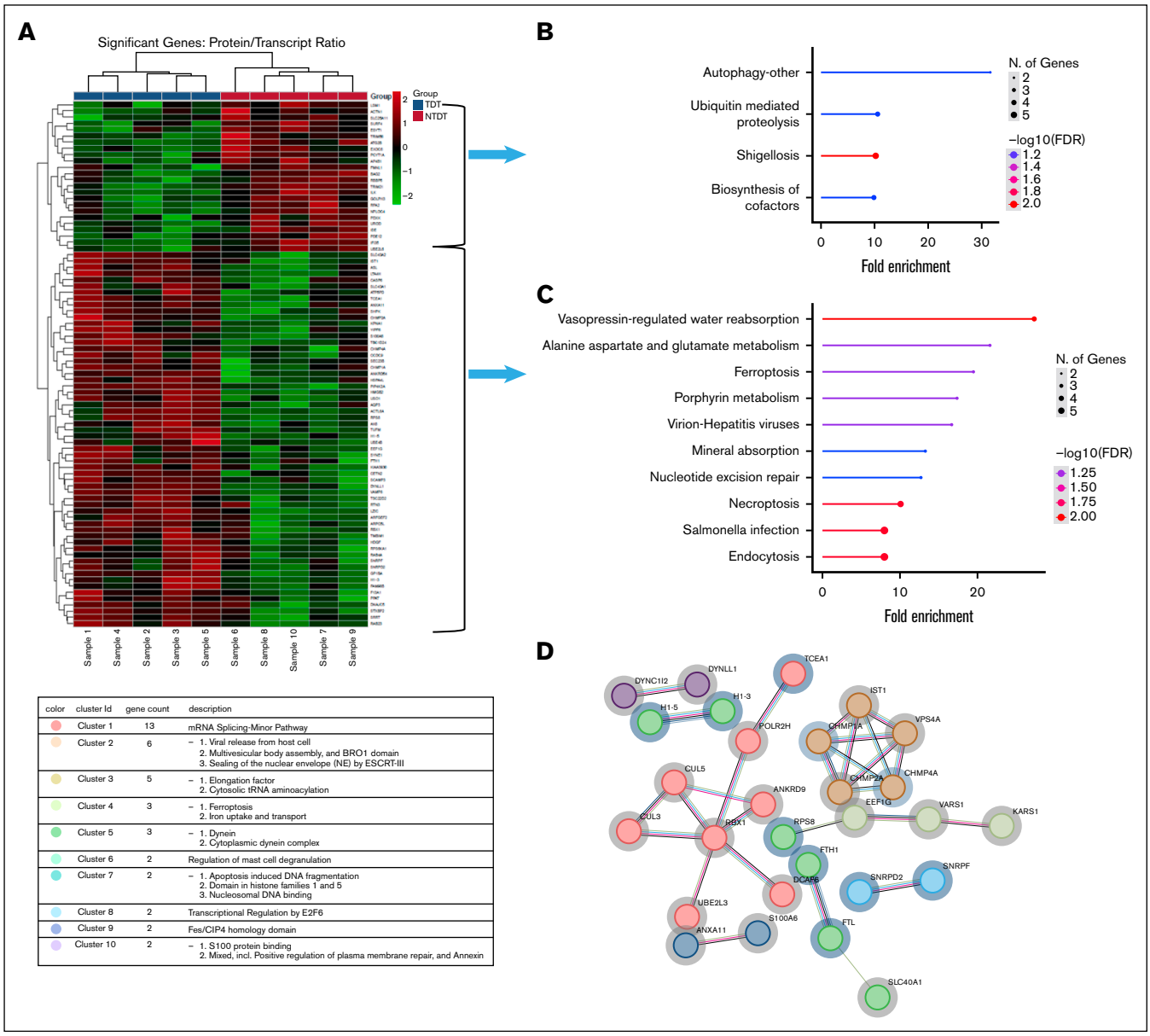

color	cluster Id	gene count	description
	Cluster 1	13	mRNA Splicing-Minor Pathway
	Cluster 2	6	– 1. Viral release from host cell 2. Multivesicular body assembly, and BRO1 domain 3. Sealing of the nuclear envelope (NE) by ESCRT-III
	Cluster 3	5	– 1. Elongation factor 2. Cytosolic tRNA aminoacylation
	Cluster 4	3	– 1. Ferroptosis 2. Iron uptake and transport
	Cluster 5	3	– 1. Dynein 2. Cytoplasmic dynein complex
	Cluster 6	2	Regulation of mast cell degranulation
	Cluster 7	2	– 1. Apoptosis induced DNA fragmentation 2. Domain in histone families 1 and 5 3. Nucleosomal DNA binding
	Cluster 8	2	Transcriptional Regulation by E2F6
	Cluster 9	2	Fes/CIP4 homology domain
	Cluster 10	2	– 1. S100 protein binding 2. Mixed, incl. Positive regulation of plasma membrane repair, and Annexin

Figure 6. PTR analysis in TDT vs NTDT samples. (A) Heat map showing hierarchical clustering of significant gene pairs based on low and high PTRs. (B-C) KEGG pathway enrichment analysis of genes with low and high PTRs, highlighting distinct pathway associations. (D) K-means clustering analysis using STRING identified 8 enriched clusters of high PTR gene signatures and their associated pathways.

networks aimed at mitigating globin chain precipitation, hemichrome toxicity, and premature RBC degradation.[27]

Conversely, downregulated transcripts were enriched for actin filament-binding and phosphoprotein-binding functions, indicating cytoskeletal fragility and reduced deformability, key contributors to hemolysis and splenic sequestration. The current proteomic findings support previous reports of membrane deformities and altered mechanical stability as major determinants of RBC fragility in β-thalassemia.[28]

Comparative transcriptomics between TDT and NTDT revealed that upregulated genes in TDT (C4BPA, CD300H, CLDN5) were enriched for TLR and RAGE binding, implicating chronic sterile inflammation as a key modifier of disease severity. Heme-induced activation of RAGE and TLR pathways is known to trigger inflammatory apoptosis, exacerbating ineffective erythropoiesis.[29] GSEA confirmed elevated apoptotic signatures and reduced hematopoietic lineage expression in TDT, consistent with suppression of erythroid maturation. Collectively, these results indicate that inflammation-driven oxidative and apoptotic stress amplify erythroid destruction in TDT.

Proteomic profiling by MS identified extensive remodeling of the RBC proteome, with 826 proteins significantly altered between the thalassemia and control groups. Upregulated proteins were enriched in RNA binding, translation initiation (eukaryotic initiation

factor 3 complex), and chaperone-mediated folding (HSPA1B, DNAJB4), suggesting a heightened translational and proteostatic demand in thalassemic erythroid cells. In contrast, downregulated proteins were associated with haptoglobin binding and antioxidant functions, consistent with depletion of hemoglobin-scavenging and redox-buffering mechanisms. STRING network analysis linked these proteins to hemolytic anemia–related pathways, reinforcing previous evidence of impaired detoxification and redox homeostasis in thalassemia.[30]

Between TDT and NTDT, the proteomic data further confirmed disease severity–related dysregulation, with overexpression of ferritin heavy and light chains (FTH1, FTL) linked to ferroptosis and iron overload, and upregulation of RAGE-/TLR4-interacting proteins that promote inflammation and oxidative injury. Simultaneously, reduced levels of oxygen-binding and chaperone proteins reflected impaired oxygen transport and cytoprotectant. Downregulation of autophagy and mitophagy components suggested defective clearance of damaged organelles, contributing to the accumulation of defective erythroid precursors and ineffective erythropoiesis.

Integrated multiomics correlation analysis revealed a widespread loss of mRNA-protein concordance in thalassemia compared with controls. cocor-based correlation density plots displayed a bell-shaped distribution centered near zero, indicating global uncoupling between transcriptional and translational output. CDK11A and MCTS1 exhibited positive correlations in controls but inverse patterns in thalassemia, suggesting posttranscriptional dysregulation involving RNA-binding proteins and translational repressors. In contrast, RLP38 and H3C1 shifted from negative to positive correlation, reflecting compensatory overtranslation of stress-response transcripts. Motif enrichment analysis linked these discordant genes to transcription factors ELK1, E2F4, YY1, and Sp1, key regulators of erythropoiesis and stress-adaptive translation.[31-38]

Comparison between TDT and NTDT identified 84 genes with significant differences in transcript-protein correlation. Key negatively correlated pairs (WNK3, HNRNPUL1, COPS7A, HTATSF1) showed impaired coordination in TDT. These genes participate in RNA processing, ubiquitin-mediated degradation, and vesicular trafficking, suggesting breakdowns in proteostasis and mRNA turnover associated with increased disease severity.[39-42]

Because isolation of reticulocytes from mature RBCs was technically unfeasible, we computed the PTR to integrate transcriptomic and proteomic signals. PTR provided a composite index of transcriptional activity (reticulocyte derived) and functional protein output (mature RBC derived).[14,43] In thalassemia, genes with low PTRs were enriched in cytoskeletal components (ankyrin, spectrin), indicating inefficient translation or accelerated degradation, whereas high PTRs corresponded to ribosomal and RNA-binding proteins, denoting translational stress. TDT samples exhibited higher PTRs for ferroptosis-related proteins (FTH1, FTL, heme oxygenase-1) and lower PTRs for autophagy genes, suggesting impaired cellular recycling and enhanced oxidative cell death.[44]

Collectively, these integrated findings indicate that multiple dysregulated molecular pathways converge to determine disease severity in TDT, even in the presence of an identical β^{+}/β^{0} genotype (Figure 7). The comparatively severe pathogenicity observed in the TDT group seems to arise from profound alterations in RNA processing, proteostasis, and erythroid homeostasis. A major contributor may be aberrant pre-mRNA splicing, given that disruption of snRNP and spliceosome components compromises efficient mRNA maturation. In parallel, dysregulation of post-transcriptional and translational control, together with enhanced ribosomal and chaperone activity, suggests a compensatory unfolded protein response that nevertheless fails to restore translational fidelity. Elevated ferritin expression (FTH1, FTL) coupled with reduced heme binding promotes iron-dependent

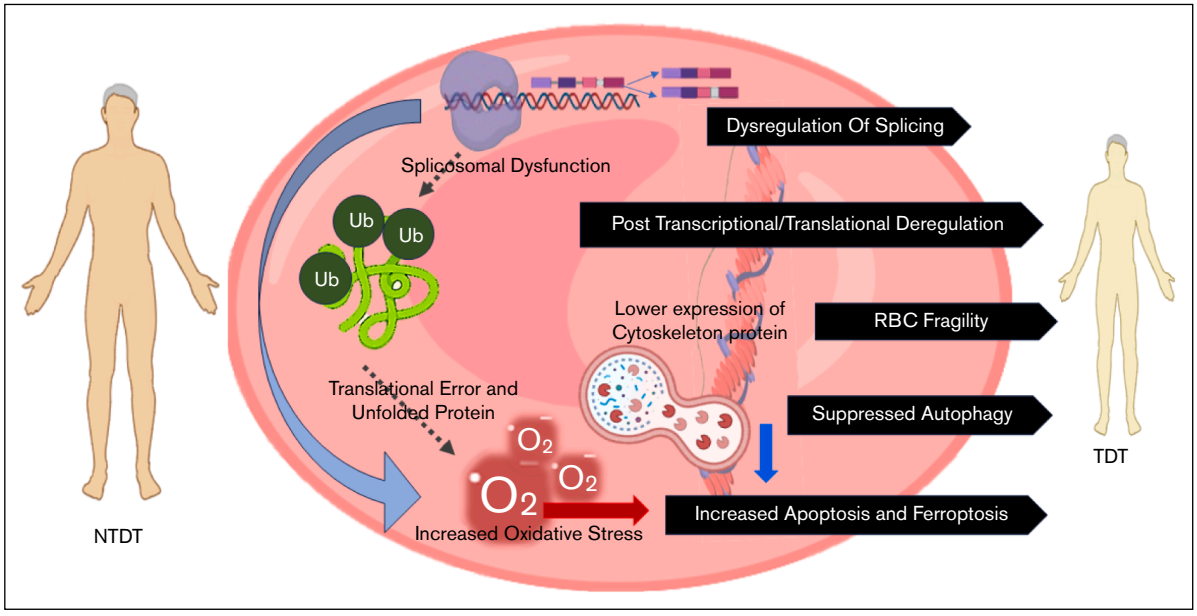

Figure 7. Schematic model for convergence of multiple dysregulated molecular pathways underlying disease severity in TDT.

oxidative injury and ferroptotic cell death, whereas impaired clearance of damaged proteins further accelerates erythrocyte loss through defective autophagy. Transcriptional overactivation of ELK1, E2F4, and Sp1 likely amplifies translational stress and apoptotic signaling. In addition, reduced cytoskeletal stability increases membrane fragility, exacerbating hemolysis. The combined impact of translational inefficiency, oxidative stress, ferroptosis, and defective erythropoiesis ultimately drives the profound anemia and transfusion dependence characteristic of TDT, whereas NTDT seems to retain partial proteostatic control that permits residual erythropoiesis.

Similar mechanistic patterns have been reported: microRNA-144/451 loss alleviates β-thalassemia via Unc-51-like kinase 1–mediated autophagy,[45] mechanistic target of rapamycin inhibition enhances mitochondrial clearance,[46] and heme-regulated inhibitor kinase modulates erythroid stress responses.[47] Thus, our integrated omics data from patient-derived RBCs confirm and extend these mechanistic insights, revealing actionable pathways that may serve as potential therapeutic targets in β-thalassemia.[48-55]

Although this genetically homogeneous cohort provides direct in vivo evidence for multilayered dysfunction in β-thalassemia RBCs, the study has certain limitations. The sample size is relatively small, and the proposed dysregulated pathways have not yet been validated through targeted functional experiments. Therefore, the current work should be viewed as a foundation that generates a priori knowledge and mechanistic hypotheses regarding pathway dysregulation and disease severity in thalassemia. Before any therapeutic targeting of these pathways is attempted, each dysregulated axis can be validated through functional assays and experimental models for further drug development studies.

Acknowledgments

The authors thank all the patients with thalassemia and control participants, the National Genomics Core, Proteomics Facility, BRIC-National Institute of Biomedical Genomics, Kalyani, India, for RNA sequencing, proteomics work and intramural funding (A.B.), and The University of Burdwan, Bardhaman, India, for necessary support.

This work was partially supported by funding from the Department of Biotechnology, Government of India (sanction no. BT/PR26461/MED/12/821/2018).

Authorship

Contribution: N.M. performed the experiments and data analyses, and drafted the manuscript; U.B. and N.M. assisted during experiments and manuscript writing; P.C. clinically investigated the patients; A.P. assisted during proteomics sample processing and instrument handling; A.K. checked the proteomics workflow and data; S.B. guided some of the statistical analyses; and A.B. designed the experiments, planned the study, checked the data, and finalized the manuscript.

Conflict-of-interest disclosure: The authors declare no competing financial interests.

ORCID profiles: N.M., 0009-0004-1380-6123; U.B., 0009-0009-2055-7870; P.C., 0000-0003-2955-7470; A.P., 0009-0005-5029-4486; A.M.K., 0000-0001-5806-3539; S.B., 0000-0002-8549-1130; A.B., 0000-0002-0608-9267.

Correspondence: Anupam Basu, Department of Zoology, The University of Burdwan, Bardhaman 713104, India; email: abasu@zoo.buruniv.ac.in.

References

1. Tuo Y, Li Y, Li Y, et al. Global, regional, and national burden of thalassemia, 1990-2021: a systematic analysis for the global burden of disease study 2021. *EClinicalMedicine*. 2024;72:102619.
2. Taher A, Vichinsky E, Musallam K, Cappellini MD, Viprakasit V, Weatherall D. *Guidelines for the Management of Non-Transfusion Dependent Thalassaemia (NTDT)*. 1st ed. Thalassaemia International Federation; 2013.
3. Saha D, Chowdhury PK, Panja A, et al. Effect of deletions in the α-globin gene on the phenotype severity of β-thalassemia. *Hemoglobin*. 2022;46(2):118-123.
4. Taher A, Weatherall DJ, Cappellini MD. Thalassaemia. *Lancet*. 2018;391(10116):155-167.
5. Taher A, Saliba AN. Iron overloading in thalassemia: different organs at different rates. *Hematol Am Soc Hematol Educ Program*. 2017;2017(1):265-271.
6. Ghosh D, Panja A, Saha D, Banerjee U, Datta AK, Basu A. Drug repurposing: hydroxyurea therapy improves the transfusion-free interval in HbE/beta-thalassemia major patients with the *XmnI* polymorphism. *Genet Test Mol Biomarkers*. 2021;25(8):563-570.
7. Cappellini MD, Viprakasit V, Taher AT, et al. Phase 3 trial of luspatercept in patients with transfusion-dependent beta-thalassemia. *N Engl J Med*. 2020;382(13):1219-1231.
8. Forsyth S, Schroeder P, Geib J, et al. Safety, pharmacokinetics, and pharmacodynamics of etavopivat (FT-4202), an allosteric activator of pyruvate kinase-R, in healthy adults: a randomized, placebo-controlled, double-blind, first-in-human phase 1 trial. *Clin Pharmacol Drug Dev*. 2022;11(5):654-665.
9. Jain V, Yang WH, Wu J, Roback JD, Gregory SG, Chi JT. Single-cell RNA-seq analysis of human red cells. *Front Physiol*. 2022;13:828700.
10. Sangokoya C, LaMonte G, Chi JT. Isolation and characterization of microRNAs of human mature erythrocytes. *Methods Mol Biol*. 2010;667:193-203.
11. Kannan M, Atreya C. Differential profiling of human red blood cells during storage for 52 selected microRNAs. *Transfusion*. 2010;50(7):1581-1588.
12. Gautier EF, Ducamp S, Leduc M, et al. Comprehensive proteomic analysis of human erythropoiesis. *Blood*. 2016;16(5):1470-1484.

13. Chu TTT, Sinha A, Malleret B, et al. Quantitative mass spectrometry of human reticulocytes reveals proteome-wide modifications during maturation. *Br J Haematol*. 2018;180(1):118-133.

14. Liu J, et al. Integrative analysis of transcriptome and proteome in erythroid cells reveals post-transcriptional regulation. *Blood Adv*. 2021;5(17):3381-3394.

15. Leduc M, Papoin J, Yan H, et al. Comprehensive phenotypic and proteomic analyses of human reticulocyte maturation. *Blood Red Cells Iron*. 2025;1(2):100012.

16. Farmakis D, Porter J, Taher A, Domenica Cappellini M, Angastiniotis M, Eleftheriou A. 2021 Thalassaemia International Federation guidelines for the management of transfusion-dependent thalassemia. *Hemasphere*. 2022;6(8):e732.

17. Arvind MK, Qibin Z. Comprehensive quantification of carboxymethyllysine-modified peptides in human plasma. *J Am Soc Mass Spectrom*. 2021;32(3):744-752.

18. Diedenhofen B, Musch J. cocor: a comprehensive solution for the statistical comparison of correlations. *PLoS One*. 2015;10(3):e0121945.

19. Smyth GK. Linear models and empirical Bayes methods for assessing differential expression in microarray experiments. *Stat Appl Genet Mol Biol*. 2004;3:Article3.

20. Ritchie ME, Phipson B, Wu D, et al. limma powers differential expression analyses for RNA-sequencing and microarray studies. *Nucleic Acids Res*. 2015;43(7):e47.

21. Vogel C, Marcotte EM. Insights into the regulation of protein abundance from proteomic and transcriptomic analyses. *Nat Rev Genet*. 2012;13(4):227-232.

22. Zhou Y, Zhou B, Pache L, et al. Metascape provides a biologist-oriented resource for the analysis of systems-level datasets. *Nat Commun*. 2019;10(1):1523.

23. Perez-Riverol Y, Bai J, Bandla C, et al. The PRIDE database resources: a hub for mass spectrometry-based proteomics evidences. *Nucleic Acids Res*. 2022;50(D1):D543-D552.

24. Gardenghi S, Ramos P, Roy CN, et al. Hepcidin as a therapeutic tool to limit iron overload and improve anemia in β-thalassemia. *Blood*. 2010;116(21):1009.

25. Rund D, Rachmilewitz E. Beta-thalassemia. *N Engl J Med*. 2005;353(11):1135-1146.

26. Strader MB, Kassa T, Meng F, et al. Oxidative instability of hemoglobin E (β26 Glu→Lys) is increased in the presence of free α subunits and reversed by α-hemoglobin stabilizing protein (AHSP): relevance to HbE/β-thalassemia. *Redox Biol*. 2016;8:363-374.

27. Longo F, Piolatto A, Ferrero GB, Piga A. Ineffective erythropoiesis in beta-thalassemia: key steps and therapeutic options by drugs. *Int J Mol Sci*. 2021;22(13):7229.

28. Barshtein G, Pajic-Lijakovic I, Gural A. Deformability of stored red blood cells. *Front Physiol*. 2021;12:722896.

29. May O, Yatime L, Merle NS, et al. The receptor for advanced glycation end products is a sensor for cell-free heme. *FEBS J*. 2021;288(11):3448-3464.

30. Khandros E, Thom CS, D'Souza J, Weiss MJ. Integrated protein quality-control pathways regulate free α-globin in murine β-thalassemia. *Blood*. 2012;119(22):5265-5275.

31. Kinross KM, Clark AJ, Iazzolino RM, Humbert PO. E2F4 regulates fetal erythropoiesis through the promotion of cellular proliferation. *Blood*. 2006;108(3):886-895.

32. Perreault AA, Brown JD, Venters BJ. Erythropoietin regulates transcription and YY1 dynamics in a pre-established chromatin architecture. *iScience*. 2020;23(10):101583.

33. Xi H, Yu Y, Fu Y, Foley J, Halees A, Weng Z. Analysis of overrepresented motifs in human core promoters reveals dual regulatory roles of YY1. *Genome Res*. 2007;17(6):798-806.

34. Gille H, Strahl T, Shaw PE. Activation of ternary complex factor Elk-1 by stress-activated protein kinases. *Curr Biol*. 1995;5(10):1191-1200.

35. Zhang Y, Zhou Y, Li X, et al. Small-molecule α-lipoic acid targets ELK1 to balance human neutrophil and erythrocyte differentiation. *Stem Cell Res Ther*. 2024;15(1):100.

36. Gilmour J, O'Connor L, Middleton CP, et al. Robust hematopoietic specification requires the ubiquitous Sp1 and Sp3 transcription factors. *Epigenetics Chromatin*. 2019;12(1):33.

37. Bacon ER, Dalyot N, Filon D, Schreiber L, Rachmilewitz EA, Oppenheim A. Hemoglobin switching in humans is accompanied by changes in the ratio of the transcription factors GATA-1 and SP1. *Mol Med*. 1995;1(3):297-305.

38. Li Z, Schulz MH, Look T, Begemann M, Zenke M, Costa IG. Identification of transcription factor binding sites using ATAC-seq. *Genome Biol*. 2019;20(1):45.

39. Long Y, Ren Y, Wei Q, et al. NAT_{10}-mediated RNA acetylation enhances HNRNPUL1 mRNA stability to contribute to cervical cancer progression. *Int J Med Sci*. 2023;20(8):1079-1090.

40. Corsini NS, Knoblich JA. Coordinated control of mRNA and rRNA processing controls embryonic stem cell pluripotency and differentiation. *Cell Stem Cell*. 2018;22(4):543-558.

41. Du W, Xu Y, et al. Targeting the COP9 signalosome for cancer therapy. *Cancer Biomed*. 2022;19(5):573-590.

42. Boyd-Shiwarski C, Shiwarski DJ, Griffiths SE, et al. WNK kinases sense molecular crowding and rescue cell volume via phase separation. *Cell*. 2022;185(24):4488-4506.

43. Boussaid I, Le Goff S, Floquet C, et al. Integrated analyses of translatome and proteome identify the rules of translation selectivity in RPS14-deficient cells. *Haematologica*. 2021;106(3):746-758.

44. Martínez-García GG, Pérez RF, Fernández ÁF, Durand S, Kroemer G, Mariño G. Autophagy deficiency by Atg4B loss leads to metabolomic alterations in mice. *Metabolites*. 2021;11(8):481.

45. Keith J, Christakopoulos GE, Fernandez AG, et al. Loss of miR-144/451 alleviates β-thalassemia by stimulating ULK1-mediated autophagy of free α-globin. *Blood*. 2023;142(10):918-932.

46. Liu Q, Hao T, Lin Z, et al. AZD8055 is more effective than rapamycin in inhibiting proliferation and promoting mitochondrial clearance in erythroid differentiation. *Anal Cell Pathol (Amst)*. 2024;2024:2639464.

47. Ricketts MD, Emptage RP, Blobel GA, Marmorstein R. The heme-regulated inhibitor kinase requires dimerization for heme-sensing activity. *J Biol Chem*. 2022;298(10):102451.

48. Makis A, Hatzimichael E, Papassotiriou I, Voskaridou E. Clinical trials update in new treatments of β-thalassemia. *Am J Hematol*. 2016;91(11):1135-1145.

49. Matte A, Federti E, Winter M, et al. Bitopertin, a selective oral GLYT1 inhibitor, improves anemia in a mouse model of β-thalassemia. *JCI Insight*. 2019;4(22):e130111.

50. Michels AA, Fraldi A, Li Q, et al. Binding of the 7SK snRNA turns the HEXIM1 protein into a P-TEFb (CDK9/cyclin T) inhibitor. *EMBO J*. 2004;23(13):2608-2619.

51. Carvalho T, Martins S, Rino J, Marinho S, Carmo-Fonseca M. Pharmacological inhibition of the spliceosome subunit SF3b triggers exon junction complex-independent nonsense-mediated decay. *J Cell Sci*. 2017;130(9):1519-1531.

52. Macri C, Wang F, Tasset I, et al. Modulation of deregulated chaperone-mediated autophagy by a phosphopeptide. *Autophagy*. 2015;11(3):472-486.

53. Zheng W, Qian Y, Chen S, Ruan H, Fan C. Rapamycin protects against peritendinous fibrosis through activation of autophagy. *Front Pharmacol*. 2018;9:402.

54. Wortmann L, Bräuer N, Holton SJ, et al. Discovery and characterization of potent and highly selective 1,7-naphthyridine-based inhibitors BAY-091 and BAY-297 of the kinase PIP4K2A. *J Med Chem*. 2021;64(21):15883-15911.

55. Tong J, Lan XT, Zhang Z, et al. Ferroptosis inhibitor liproxstatin-1 alleviates metabolic dysfunction-associated fatty liver disease in mice: potential involvement of PANoptosis. *Acta Pharmacol Sin*. 2023;44(5):1014-1028.